DOI: 10.1002/anie.200803773

Nanoparticle Catalysts

Preparation of Rhodium Nanoparticles in Carbon Dioxide Induced Ionic Liquids and their Application to Selective Hydrogenation**

Valentin Cimpeanu, Marijan Kočevar, Vasile I. Parvulescu, and Walter Leitner**

There is currently great interest in the generation of metal nanoparticles of controlled size and shape because of their unique properties at the interface between molecular structures and bulk materials.[1,2] Ionic liquids (ILs) have emerged as promising media for the synthesis, stabilization, and utilization of metal nanoparticles for various applications, including catalysis.[3,4] The stabilizing effect of ammonium salts on metal nanoparticles is well-established in conventional solvents[1,2,5] and is of course not restricted to materials with melting points that fall within the definition of ILs (that is, organic salts with melting points, T_m, below 100 °C[6]). Most recently, it has been demonstrated that common organic salts can experience very significant melting point depression in the presence of compressed CO_2 with ΔT_m values around or above 100 °C in certain cases.[7,8] Herein, we report a method for the generation and entrapment of rhodium nanoparticles in simple solid ammonium salts by exploiting their CO_2-induced melting to form ionic liquids. The utilization of the resulting materials as selective catalysts for hydrogenation reactions is exemplified, whereby a different catalytic behavior from conventional homogeneous or heterogeneous catalysts was noted for sterically encumbered aromatic olefins as substrates.

The process for the generation of the matrix-embedded nanoparticles is depicted in Figure 1. A mixture of the solid ammonium salt $[R_4N]Br$ and the organometallic complex $[Rh(acac)(CO)_2]$ (acac = acetylacetonate) as precursor (Rh loading ca. 1 % by weight) is placed into a window-equipped autoclave. This mixture is then pressurized with CO_2 and H_2 and heated to 40–80 °C for the reduction step. Although most simple ammonium salts have regular melting points around or well above 100 °C, they form liquid phases under the reaction conditions because of the presence of the compressed CO_2 phase.[7,8] This ensures the dissolution of the molecular precursor and a homogeneous dispersion of the resulting particles. Furthermore, the presence of CO_2 is known to enhance the availability of hydrogen in ionic-liquid phases, which may further facilitate the reduction process.[9] Upon venting the CO_2/H_2 mixture at the end of the reaction, the nanoparticles are trapped in the solidifying matrix that is left in the reactor.

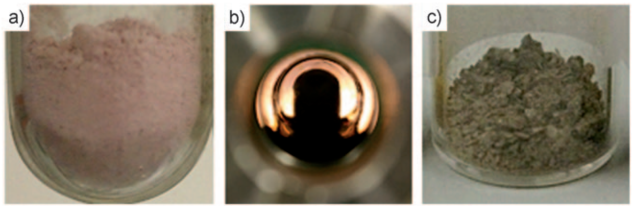

Figure 1. Generation of matrix-embedded rhodium nanoparticles by reduction in CO_2-induced ionic liquids. a) Mixture of the ammonium salt and solid molecular precursor complex $[Rh(acac)(CO)_2]$; b) reduction under CO_2/H_2 in the CO_2 induced ionic liquid phase (view into the high pressure reactor including the magnetic stirrer bar); c) solid material containing the embedded nanoparticles obtained after venting the reactor.

Organic by-products are inevitably formed from the ligands during the preparation of metal nanoparticles by hydrogenation of organometallic precursor complexes. Such side products can be readily removed from the resulting material by extraction with supercritical CO_2 ($scCO_2$). This was demonstrated in the present method by passing a $scCO_2$ stream through the reactor after reduction and venting through an indicator solution of $Fe_2(SO_4)_3$ (1 % in H_2SO_4 (0.1 N)). The immediate appearance of the characteristic red color of $[Fe(acac)_3]$ proved the presence of acetylacetone in the CO_2 flow.

With this simple procedure, well-defined rhodium nanoparticles were obtained in various ionic matrices at mild temperatures as exemplified for three different ammonium

---

[*] Dr. V. Cimpeanu, Prof. Dr. W. Leitner
Institut für Technische und Makromolekulare Chemie
RWTH Aachen, Worringerweg 1, 52074 Aachen (Germany)
Fax: (+49) 241-802-2177
E-mail: leitner@itmc.rwth-aachen.de
Homepage: http://www.itmc.rwth-aachen.de

Prof. Dr. W. Leitner
Max-Planck-Institut für Kohlenforschung
Kaiser-Wilhelm-Platz 1, 45470 Mülheim an der Ruhr (Germany)

Prof. Dr. V. I. Parvulescu
Department of Chemical Technology and Catalysis
University of Bucharest
B-dul Regina Elisabeta 4-12, 030016 Bucharest (Romania)
E-mail: v_parvulescu@yahoo.com

Prof. Dr. M. Kočevar
Faculty of Chemistry and Chemical Technology
University of Ljubljana (Slovenia)

[**] This work was supported by the Deutsche Forschungsgemeinschaft (SPP 1191 "Ionic Liquids", grant no. LE 930/11) and the Fonds der Chemischen Industrie. We thank Dr. B. Tesche and Axel Dreier (Max-Planck-Institut für Kohlenforschung, Mülheim am der Ruhr) for TEM measurements and Dr. Robert Kaufmann (Deutsches Wollforschunginstitut, RWTH Aachen) for XPS spectra. The Alexander von Humboldt Foundation is gratefully acknowledged for making this collaboration possible through a fellowship to V.I.P.

Supporting information for this article is available on the WWW under http://dx.doi.org/10.1002/anie.200803773.

bromide salts and the resulting materials **Rh-1** to **Rh-3** (Table 1; for further examples see the Supporting Information). The brownish solid particles could be redissolved under pressurized CO_2 to form homogeneous solutions. Even after storage of the solids over three months, the nanoparticles in **Rh-1** to **Rh-3** remained stable and no change in their catalytic behavior was observed. Consistent with other ammonium halide stabilized nanoparticles,[10] typical particle sizes of the homogenously dispersed clusters were in the range 1–4 nm, with relatively narrow distributions in most cases, as determined from TEM micrographs (Figure 2a).

Table 1: Selected characteristic data for rhodium nanoparticles embedded in solid ammonium salts that were generated by CO_2-induced ionic liquid phases.[a]

Cat.	Matrix	M.p. [°C]	T [°C]	p[b] [bar]	Particle size [nm]	Surface/bulk atom ratio	Rh^0/Rh^I ratio[c]
Rh-1	$[Bu_4N]Br$	124[d]	80	240	3.3 ± 1.5	0.33	0.63
Rh-2	$[Hex_4N]Br$	100[d]	40	150	2.3 ± 0.8	0.47	0.62
Rh-3	$[Oct_4N]Br$	98[c]	60	220	1.4 ± 0.3	0.78	0.59

[a] Reaction conditions: ionic matrix (0.5 g), precursor $[Rh(acac)(CO)_2]$ (1 % Rh), H_2 (40 bar), and $scCO_2$ (density: ca. 0.7 g mL^{-1}), 180 min. [b] Total pressure at reduction temperature. [c] Calculated by using XPS. [d] Melting points of the pure matrix under standard conditions.

X-ray photoelectron spectroscopic (XPS) analysis of the new materials **Rh-1** to **Rh-3** showed the characteristic signals for the matrix[11] and the embedded rhodium nanoparticles (Figure 2b,c).[12] Deconvolution of the signals corresponding to the Rh $3d_{5/2}$ level revealed two components; the minor component is centered around 307.2 eV and can be assigned to fully reduced Rh^0 centers.[13] The binding energies of the major signal are in the range 308.0–308.3 eV, that is between the value of the Rh^I precursor ($[Rh(acac)(CO)_2]$, 309.2 eV[14]) and of reduced Rh^0 species. Such values are typical for small rhodium nanoparticles and indicate a partial oxidation to Rh^I.[14]

The matrix-embedded nanoparticles **Rh-1** to **Rh-3** can be used directly for catalytic hydrogenation reactions without any further workup or purification. This was demonstrated by first using cyclohexene (**1**) and benzene (**2**) as test substrates under a standard set of reaction conditions (Table 2). The catalyst materials were suspended or partly dissolved in the neat substrate and hydrogen uptake was monitored online. Turnover frequency (TOF) values were determined from the slope within the first 20 % of conversion. The reactions were stopped after 30 minutes for **1** and after 120 minutes for **2**, and offline GC analysis confirmed quantitative conversion to **3** at this stage. TOF values for the hydrogenation of **1** in the range of $10^4\,h^{-1}$ were observed with all materials under neat conditions. Reaction rates were about two orders of magnitude lower for the reduction of the aromatic substrate **2**. These data are consistent with previously reported rates obtained with rhodium nanoparticles in standard ionic liquids.[4a]

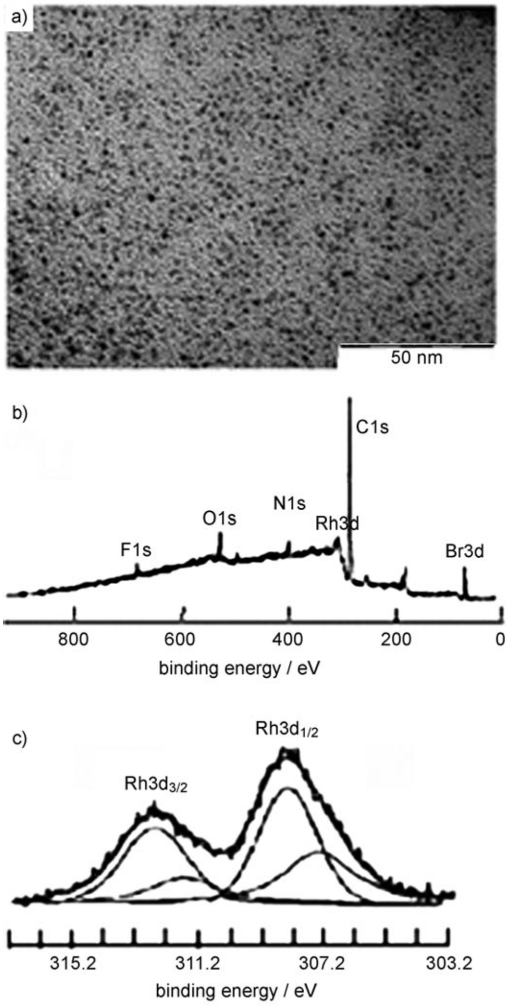

Figure 2. a) Representative TEM micrograph (scale bar = 50 nm). b) Overview and c) expansion of the rhodium signals in XPS spectra of rhodium nanoparticles generated from $[Rh(acac)(CO)_2]$ in $[Hex_4N]Br$ (**Rh-2**).

Material **Rh-1** was insoluble in nonpolar media and could be readily separated and recycled by extraction with pentane. The turnover frequency value corrected for surface-exposed rhodium centers ($TOF_{surface}$) dropped slightly after the first run, but then remained stable at a value of approximately 14300 h^{-1} for at least four more runs. TEM micrographs and XPS of a sample after three catalytic cycles indicated that the primary particles remained largely unchanged (particle size: (2.6 ± 0.6) nm), although some partial agglomeration was indicated by the TEM images and UV/Vis spectra. The other materials were at least partially soluble in the reaction mixtures, but could be readily precipitated and recovered in active form by extraction of the products with $scCO_2$.[15,16]

The promising results obtained with the simple test reactions prompted us to evaluate the new materials as catalysts for more challenging substrates. The sterically encumbered (*E*)-2-(benzoylamino)-2-propenoic acid derivatives **4a**–**e** (Scheme 1) are precursors for nonnatural amino acids and show interesting biological activities.[17] Selective hydrogenation would be an interesting transformation to

Table 2: Representative catalytic results for benchmark hydrogenation reactions using matrix-embedded rhodium nanoparticles.[a]

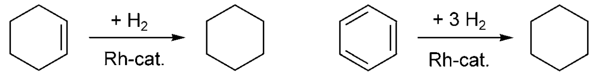

1 **3** **2** **3**

Cat.	Phase behavior	TOF_{total} $[h^{-1}]$[b]	$TOF_{surface}$ $[h^{-1}]$[c]	Phase behavior	TOF_{total} $[h^{-1}]$[b]	$TOF_{surface}$ $[h^{-1}]$[c]
Rh-1	immiscible	8800	26650	partially miscible	35	106
Rh-2	partially miscible	6600	14050	partially miscible	8	17
Rh-3	partially miscible	35700	45800	partially miscible	42	54

[a] Reaction conditions: $T = 40\,°C$, $p(H_2) = 40$ bar, neat; **1**: Rh = 1000:1, **2**: Rh = 100:1. [b] Total turnover frequency determined as mol substrate per total amount of rhodium in matrix per hour, determined from hydrogen uptake within the first 20% conversion; full conversion was reached in all cases after appropriate reaction time. [c] Turnover frequency corrected for surface-exposed rhodium centers by using the dispersion data from Table 1.

increase the structural diversity of these substances (Scheme 1). However, typical homogeneous rhodium catalysts such as Wilkinson's catalyst do not show any hydrogenation activity for these substrates at temperatures and pressures below their decomposition (< 5% conversion after 3 days at 120 °C and 100 bar). Use of commercial Rh/Al_2O_3 as a prototypical heterogeneous catalyst led to a quantitative conversion under these conditions, but both the olefinic double bond and the aromatic ring in the benzoyl protecting group were fully hydrogenated to give **7a–e** as the main products. Monitoring the reaction by using offline GC showed that both groups are hydrogenated with similar rates from the beginning of the reaction, and it was not possible to achieve significant selectivities for products of either type **5** or **6**.

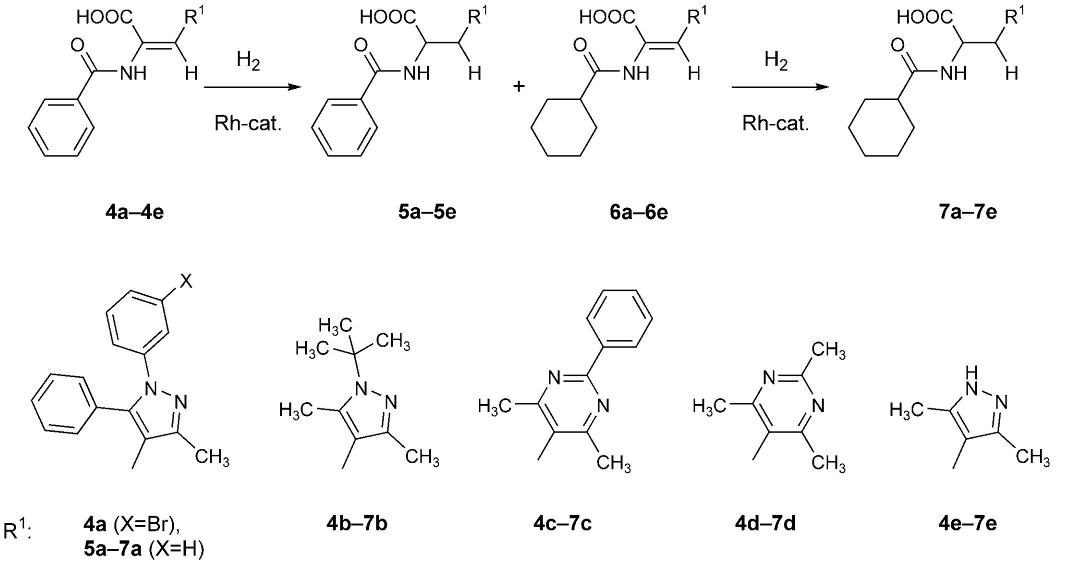

Scheme 1. Product spectrum for hydrogenation of (*E*)-2-(benzoylamino)-2-propenoic acids **4a–e**.

In contrast to the conventional catalysts, ammonium halide stabilized rhodium nanoparticles were found to combine good catalytic activities with significant differentiation between the aromatic and olefinic moieties (Table 3). In general, the hydrogenation rates are somewhat smaller over **Rh-1** than over the commercial Rh/Al_2O_3 catalyst at comparable loading. For substrates **4a–b**, all three possible hydrogenation products were formed in a network of parallel and consecutive hydrogenation processes. Remarkably, product **6b** was formed preferentially over **5b**, which indicated that hydrogenation of the aromatic moiety is faster than that of the olefinic double bond in this case. This trend is even more pronounced for the sterically more encumbered substrates **4c–d**. Product **6d** was obtained with excellent selectivity reaching up to 96% at 60% conversion. In contrast, substrate **4e**, which contains a basic NH group in the heteroaromatic substituent, was hydrogenated exclusively at the double bond to provide the benzoyl amino acid **5e** in good yields.

Table 3: Selective hydrogenation of (*E*)-2-(benzoylamino)-2-propenoic acids **4a–e** using **Rh-1** as catalyst.[a]

Substrate	*T* [°C]	TOF_{total}[b] [×10, h^{-1}]	$TOF_{surface}$[c] [×10, h^{-1}]	Selectivity[d] **5a–e**	**6a–e**	**7a–e**
4a[e]	120	70	210	39	24	37
4b	80	1550	4690	30	54	16
4c	60	50	150	6	57	38
4d	60	160	485	4	96	–
4e	80	10	30	100	–	–

[a] Reaction conditions: **4** (Rh = 500:1), *i*PrOH, H_2 (100 bar). [b] Total turnover frequency determined as mol substrate per total amount of rhodium in the matrix per minute at 20–35% conversion. [c] Turnover frequency corrected for surface-exposed rhodium centers by using the dispersion data from Table 1. [d] Determined by using GC for comparable conversions around 60%. [e] Debromination at the remote aromatic ring occurred under hydrogenation conditions with **Rh-1** and Rh/Al_2O_3.

In summary, we have shown that CO_2-induced melting to form ionic liquids provides a solvent-free approach to the generation and application of catalytically active nanoparticles entrapped and stabilized in simple ammonium halide salts. The use of the $scCO_2$ phase has several advantages during the preparation process: firstly, the CO_2-induced melting-point depression greatly expands the range of organic salts that can be employed as stabilizing matrices and secondly, organic byproducts from the molecular precursor can be removed efficiently by extraction into supercritical fluids. In catalytic applications, the obtained Rh nanoparticles showed a significantly distinct behavior as compared with standard homogeneous or heterogeneous catalysts and were readily separated and recycled from the reaction mixtures.

Experimental Section

Safety Precaution: Working with compressed gases can be hazardous and must be conducted only with suitable apparatus.

Synthesis of **Rh-1**: Tetrabutylammonium bromide (0.5 g, 1.54 mmol) and [Rh(acac)(CO)$_2$] (12.5 mg, 4.86×10^{-2} mmol, corresponding to 5 mg Rh) were placed in a 10 mL stainless-steel high-pressure reactor. The reactor was evacuated three times, pressurized to 40 bar with H$_2$ followed by CO$_2$ (ca. 7 g) using a compressor. The autoclave was heated to 80 °C, at which temperature the total pressure reached about 240 bar. A deeply colored liquid phase in equilibrium with a colorless supercritical phase was formed under these conditions. After stirring for 3 h, the reactor was cooled to ambient temperature and carefully vented. The purification step was performed at 80 °C with a constant flow of CO$_2$ (180 bar) until no acetylacetone was observed in the scCO$_2$ stream. After cooling and final depressurization, the dark-brown solid was used directly for catalysis or transferred to a Schlenk tube for further storage, analysis, and catalytic application. The materials **Rh-2** and **Rh-3** were obtained by using the same procedure (see Table 1).

General procedures for catalytic hydrogenation: Hydrogenation of cyclohexene (**1**) and benzene (**2**) (200 μL, ca. 2 mmol) were performed using **Rh-1** (20 mg, 1.94 μmol Rh) in an autoclave heated on a metal block at 40 °C, allowing 30 min for temperature equilibration before pressurization with H$_2$ (40 bar). The products were isolated by filtration or extraction with scCO$_2$ and analyzed by GC.

The hydrogenation of substrates **4a–e** (0.1 mmol) was performed using **Rh-1** (20 mg, 1.94 μmol Rh) and *i*PrOH (1 mL) in an autoclave heated on a metal block at temperatures between 60–120 °C, allowing 30 min for equilibration before pressurization with H$_2$ (100 bar). In this case, the products were isolated by column chromatography on silica gel using mixtures of EtOAc and *i*PrOH as eluents and analyzed by ^{1}H and ^{13}C NMR spectroscopy.

Received: July 31, 2008

Keywords: carbon dioxide · heterogeneous catalysis · ionic liquids · nanostructures · supercritical fluids

---

[1] *Nanoparticles. From Theory to Applications* (Ed.: G. Schmid), Wiley-VCH, Weinheim, **2004**.

[2] For selected recent reviews, see: a) J. D. Aiken III, R. G. Finke, *J. Mol. Catal. A* **1999**, *145*, 1–44; b) H. Bönnemann, R. M. Richards, *Eur. J. Inorg. Chem.* **2001**, 2455–2480; c) A. Roucoux, J. Schultz, H. Patin, *Chem. Rev.* **2002**, *102*, 3757–3778; d) M. Moreno-Manas, R. Pleixats, *Acc. Chem. Res.* **2003**, *36*, 638–643; e) M. T. Reetz, J. G. de Vries, *Chem. Commun.* **2004**, 1559–1563; f) C. Burda, X. Chen, R. Narayanan, M. A. El-Sayed, *Chem. Rev.* **2005**, *105*, 1025–1102; g) D. Astruc, F. Lu, J. R. Aranzaes, *Angew. Chem.* **2005**, *117*, 8062–8083; *Angew. Chem. Int. Ed.* **2005**, *44*, 7852–7872; h) B. Chaudret, *Top. Organomet. Chem.* **2005**, *16*, 233–259.

[3] A. Roucoux, K. Philippot in *Handbook of Homogeneous Hydrogenation* (Eds.: J. G. De Vries and C. Elsevier), Wiley-VCH, Weinheim, **2007**, pp. 217–256.

[4] a) J. Dupont, G. S. Fonseca, A. P. Umpierre, P. F. P. Fichtner, S. R. Teixeira, *J. Am. Chem. Soc.* **2002**, *124*, 4228–4229; b) M. Antonietti, D. Kuang, B. Smarsly, Y. Zhou, *Angew. Chem.* **2004**, *116*, 5096–5100; *Angew. Chem. Int. Ed.* **2004**, *43*, 4988–4992; c) D. Zhao, Z. Fei, T. Geldbach, R. Scopelliti, P. J. Dyson, *J. Am. Chem. Soc.* **2004**, *126*, 15876–15882; d) L. S. Ott, M. L. Cline, M. Deetlefs, K. R. Seddon, R. G. Finke, *J. Am. Chem. Soc.* **2005**, *127*, 5758–5759; e) G. Clavel, J. Larionova, Y. Guari, C. Guerin, *Chem. Eur. J.* **2006**, *12*, 3798–3804; f) Y. S. Chung, J. Y. Shin, C. E. Song, S.-g. Lee, *Chem. Commun.* **2008**, 942–944; g) G. A. Somorjai, F. Tao, J. Y. Park, *Top. Catal.* **2008**, *47*, 1–14; h) R. Umeda, A. Ryuhei, N. Hiroshi, T. Nakahodo, H. Fujihara, *J. Am. Chem. Soc.* **2008**, *130*, 3240–3241; i) B. Léger, A. Denicourt-Nowicki, A. Roucoux, H. Olivier-Bourbigou, *Adv. Synth. Catal.* **2008**, *350*, 153–159.

[5] a) J. Kiwi, M. Grätzel, *J. Am. Chem. Soc.* **1979**, *101*, 7214–7217; b) H. Bönnemann, W. Brijoux, R. Brinkmann, E. Dinjus, T. Joussen, B. Korall, *Angew. Chem.* **1991**, *103*, 1344–1346; *Angew. Chem. Int. Ed. Engl.* **1991**, *30*, 1312–1314; c) M. T. Reetz, W. Helbig, *J. Am. Chem. Soc.* **1994**, *116*, 7401–7402.

[6] *Ionic Liquids in Synthesis* (Eds.: P. Wasserscheid and T. Welton), Wiley-VCH, Weinheim, **2008**.

[7] For earlier reports on moderate melting-point depressions in IL/CO$_2$ systems, see S. G. Kazarian, N. Sakellarios, C. M. Gordon, *Chem. Commun.* **2002**, 1314–1315.

[8] a) A. Scurto, W. Leitner, *Chem. Commun.* **2006**, 3681–3683; b) A. M. Scurto, E. Newton, R. R. Weikel, L. Draucker, J. Hallett, C. L. Liotta, W. Leitner, C. A. Eckert, *Ind. Eng. Chem. Res.* **2008**, *47*, 493–501.

[9] M. Solinas, A. Pfaltz P. G. Cozzi, W. Leitner, *J. Am. Chem. Soc.* **2004**, *126*, 16142–16147.

[10] M. T. Reetz, W. Helbig, S. A. Quaiser, U. Stimming, N. Breuer, R. Vogel, *Science* **1995**, *267*, 367–369.

[11] E. F. Smith, I. J. Villar Garcia, D. Briggs, P. Licence, *Chem. Commun.* **2005**, 5633–5635.

[12] J. Rothe, J. Pollmann, R. Franke, J. Hormes, H. Bönnemann, W. Brijoux, K. Siepen, J. Richter, *Fresenius J. Anal. Chem.* **1996**, *355*, 372–374.

[13] *Practical Surface Analysis by Auger and X-Ray Photoelectron Spectroscopy* (Eds.: D. Briggs and M. P. Seah), Wiley, Chichester, **1983**, p. 612.

[14] J. Evans, B. E. Hayden, M. A. Newton, *Surf. Sci.* **2000**, *462*, 169–180.

[15] Of course, distillation would also allow the isolation of cyclohexane in the present examples. However, extraction with scCO$_2$ from ILs is known to be a more general isolation method allowing also the separation of low volatility products, see a) L. A. Blanchard, D. Hancu, E. J. Beckmann, J. Brennecke, *Nature* **1999**, *399*, 28–29; b) L. A. Blanchard, J. F. Brennecke, *Ind. Eng. Chem. Res.* **2001**, *40*, 287–292.

[16] For a similar precipitation–recycling of PEG-stabilized Co-nanoparticles in Pauson–Khand reactions with scCO$_2$, see J.-L. Muller, J. Klankermayer, W. Leitner, *Chem. Commun.* **2007**, 1939–1941.

[17] a) U. Schmidt, A. Lieberknecht, J. Wild, *Synthesis* **1988**, 159–1972; b) C. Bonauer, T. Walenzyk, B. König, *Synthesis* **2006**, 1–20.